



Schlussbericht 14. September 2011

Studies of particulate matter (PM) deposited in diesel particulate filters operating with biofuel, diesel fuel and fuel blends

Teil des Projekts „Einfluss der Biokomponenten (FAME) auf Emissionen und die Abgasnachbehandlungssysteme der Nutzfahrzeug-Dieselmotoren (BioExDi)“

Auftraggeber:

Bundesamt für Energie BFE
Forschungsprogramm Verbrennung
CH-3003 Bern
www.bfe.admin.ch

Kofinanzierung:

Forschungsfonds der Erdölvereinigung, CH-8001 Zürich
BAFU Sektion Luftreinhaltung, CH-3003 Bern

Industriepartner:

Hug Engineering, CH-8352 Elsau
Huss Umwelttechnik GmbH, Nürnberg (D)
Dinex Group, Middelfart (DK)

Auftragnehmer:

EMPA Materials Science and Technology
Ueberlandstrasse 129
CH-8600 Dübendorf
www.empa.ch

Autoren:

Anthi Liati, EMPA Dübendorf, Abteilung Verbrennungsmotoren
anthi.liati@empa.ch

Panayotis Dimopoulos Eggenschwiler, EMPA Dübendorf, Abteilung Verbrennungsmotoren
panayotis.dimopoulos@empa.ch

BFE-Bereichsleiter: Sandra Hermle

BFE-Programmleiter: Stephan Renz

BFE-Vertrags- und Projektnummer (Verbrennung): 154222 / 103205

BFE-Vertrags- und Projektnummer (Biomasse): 154223 / 103206

Für den Inhalt und die Schlussfolgerungen ist ausschliesslich der Autor dieses Berichts verantwortlich.

Abstract

Macroscopic studies, scanning electron microscope, as well as (high resolution) transmission electron microscope research were carried out to investigate the nature and properties of particulate matter (PM) deposited in two diesel particulate filter (DPF) types made of SiC (three DPFs catalytically coated with V_2O_5/TiO_2 and three uncoated), operating with different fuels on the same engine: two DPFs (one coated, one uncoated) run with 100% rapeseed methyl ester (RME) (B100), two with 20% RME - 80% diesel (B20) and two with 100% diesel (B0). The B100-DPFs show the lowest soot deposits, opposite to B20 and B0, which exhibit abundant soot in form of cake deposited on the DPF inlet channel walls. Primary B100 soot particles range in size between 11-38 nm (mean diameter 21 nm). Their internal nanostructure indicates relatively higher oxidative reactivity compared to diesel soot. The B100-DPFs exhibit the highest ash depositions indicating that in addition to lubricating oil, the RME fuel contributes significantly to ash formation. Particles other than soot and ash in the DPFs include: (a) Al-Si-O fibres deriving from the gasket positioned on the DPF inlet surface; (b) Ca-Al-Si-O fibers from the intumescing mat enveloping the aftertreatment assembly; (c) newly formed V-O long-prismatic nanocrystals originating from the catalytic coating layer of the coated DPFs; (d) $Fe\pm Cu\pm Ni$ fragments deriving from engine wear. The size of most of these particles is smaller than the DPF pores; they may therefore escape in the atmosphere. The non-carbonaceous PM depositions consist chemically of Ca, P, Zn, Mg, S, $\pm Na$, $\pm K$ (attributed to ash), V, Ti, W (catalytic coating) and Fe, Cu, Ni (engine wear). The uncoated B100-DPF was overheated during regeneration to $T > 1200$ °C (locally possibly to ca. 2000°C), which led to alteration of PM depositions and resulted in local melting of both DPF and PM deposition material, while some new formation of SiC (moissanite) occurred.

1. Introduction

The term particulate matter (PM), when related to the diesel exhaust gas, refers mainly to soot, the carbonaceous fraction, and ash, the inorganic, non-combustible fraction. Further but minor sources of PM in the diesel exhaust gas may be fragments from different parts of the engine and/or the exhaust aftertreatment assembly (e.g., [1] and references therein). Diesel ash originates from the lubricating oil additives and, to a minor degree, from trace metals participating in the diesel fuel composition. In contrast to soot, which is to a great extent removed from the DPFs by oxidation during regeneration, the mostly inorganic ash particles remain in the DPF and accumulate inside the filter channels. This leads to a reduction of the effective filter volume and its operational lifetime. The size of both soot and ash PM in diesel exhaust ranges from micron-, sub-micron- down to the nano-scale (<50 nm) in diameter.

The use of biofuel in diesel engines has an influence on the combustion products and therefore on the PM in the exhaust gas (e.g. [2]). The studies dealing with the characteristics of PM produced during combustion of biofuel or biofuel/diesel blends is, to our knowledge, limited (e.g. [3, 4] and references therein). Therefore, the present investigation is expected to shed more light to this topic.

Within the framework of the present work, the macro- and microscopic characteristics (nature, size, morphology) of PM deposited in six DPFs are described. The DPFs were operating with the same engine on the test bench, using rapeseed methyl ester (RME) as biofuel in the following proportions: (a) two DPFs with 100% RME (referred to as B100), (b) two DPFs with a blend of 20% RME - 80% diesel fuel (referred to as B20) and (c) two DPFs with 100% diesel fuel (referred to as B0). The relevance of the PM characteristics deposited inside DPFs for the aftertreatment industry relies on the enhancement of the effectiveness of the methods applied for the minimization of the PM depositions, the possible removal of PM from the exhaust gases, as well as the optimization of the engine operating conditions.

In the present report, information is provided on the different PM deposited in the investigated DPFs regarding: (1) the identification of the various PM constituents, (2) the distribution and interrelationships of the different PM, (3) the chemical composition, as well as the morphological and structural characteristics of the different PM and (4) the internal structure of soot PM, which is related to its oxidative reactivity.

2. Technical data

2.1. Data on the investigated DPFs

Two types of DPFs produced by two different manufacturers were investigated:

1. HUG-DPFs, named 'GFM' for the tests. The following DPFs were studied: GFM1 (B0), GFM2 (B20) and GFM4 (B100).
2. HUSS-DPFs, named 'SFM', for the tests. The following DPFs were studied: SFM1 (B0), SFM2 (B20) and SFM5 (B100).

In the following, the two filter-types will be referred to as 'GFM' and 'SFM'.

A diesel oxidation catalyst (DOC) was included upstream the DPF only with the GFM4 (B100) DPF. This DOC was made of SiC with Pt as catalytic material. The DPFs were new at the start of the tests. Each DPF was shortly degreened for approximately half an hour before three identical regeneration trials of soot loading and regeneration were performed, except for B100, where only one regeneration trial was applied. Finally, care was taken to use each DPF with the same fuel-type. With each fuel-type change, the tubes to the engine were cleaned. The characteristics of the two DPF-types are summarized below, in Table 1.

Table 1 - Summary of the DPF characteristics

	Filter element	
Manufacturer of filter medium (name used for the tests)	Hug Engineering (GFM)	Huss Engineering (SFM)
Shape of filter medium	cylindrical	hexagonal
External dimensions (mm)	Ø151x300	210x203
Filter volume (dm³)	4.9	5.82
Filter total surface area (m³)	3.4	3.99
Material	SiC	SiC
Porosity (%)	48	55
Pore size (µm)	18-20	10 (mean)
Shape of cells	rectangular	triangular
Size of cells (mm)	2x2	2x2x2
Wall thickness (mm)	0.3	0.35
Number of cells/in² (CPSI)	100	200
Maximum operating T (°C)	600	1200 (peak)
Storage capacity for soot/ash (g/l)	ca. 50	8-10
Catalytic coating	TiO ₂ /V2O ₅	No

All the DPFs included in the tests operated on the same engine. The engine characteristics are summarised below, in Table 2.

In the present report, the results of the study of PM depositions will be considered separately for two types of DPFs.

Table 2 – Characteristics of the engine, on which the studied DPFs operated

Manufacturer	Liebherr Machines Bulle S.A., Bulle/Fribourg
Type	D934S
Cylinder volume	6.36 Liters
Rated RPM	2000 min ⁻¹
Rated power	111 kW
Model	4 cylinder in-line
Combustion process	Direct injection
Injection pump	Bosch unit pumps
Supercharging	Turbocharger with intercooling
Emission control	none (exhaust gas aftertreatment according to the requirements)
Development period	2005

3. Operation conditions of the investigated DPFs

GFM: The DPFs were soot loaded in a rectangular cycle: 800–1100 rpm and 0–500 Nm. This cycle is characterized as ‘mixed engine operation’. Soot loading was conducted always to the same backpressure of 100 mbar. Regeneration tests were performed in an identical way: increasing the engine load (torque) in steps at a constant engine speed with 1100 rpm. The steps lasted 10 min each and the load increase was 10%.

SFM: Soot loading was performed by means of repeated load jumps in a rectangular cycle (800–1100 rpm and 0–500 Nm).

The PM-loading and regeneration conditions are summarised below, in Table 3.

Table 3: Summary of the PM loading and regeneration conditions for the tested DPFs

GFM-DPFs (coated)	B100 (GFM4)	B20 (GFM2)	B0 (GFM1)
Loading procedure	1x soot loading & regeneration	3x soot loading & regeneration	3x soot loading & regeneration
Loading time	27 h	3h, 2h45', 2h45'	2h, 1h25', 1h40'
Regeneration type	¹ passive with DOC and catalytic coating	¹ passive with catalytic coating	¹ passive with catalytic coating
SFM-DPFs (uncoated)	B100 (SFM5)	B20 (SFM2)	B0 (SFM1)
Loading procedure	1x soot loading & regeneration	3x soot loading & regeneration	3x soot loading & regeneration
Loading time	7h30'	2h30', 3h15', 2h40',	3h50', 4h, 2h50',
Regeneration type	active/standstill with burner	active/standstill with burner	active/standstill with burner
Regeneration T (°C)	>1200, locally ca. 2000	ca. 600	ca. 600

¹Minimum exhaust temperature for the beginning of regeneration: 220 °C. Maximum temperature during regeneration: ca. 450 °C.

4. Analytical techniques

For the detailed examination of PM depositions, the DPFs were first split into their segment constituents by means of a compression strength apparatus. The segments were further sectioned parallel and perpendicular to the flow direction. Part of the PM deposits in the DPFs were extracted mechanically from the inlet and/or outlet channels, while part of them were investigated *in situ*, as deposited within the DPF channels.

The study of PM was carried out by means of optical microscopy and scanning electron microscopy (SEM), in high vacuum. SEM imaging was combined with an energy dispersive X-ray system (EDX) for qualitative chemical analyses of the investigated phases. The SEM used for this study was a Hitachi S-4800 instrument at EMPA laboratories. Preliminary data on the nanostructure of the soot were obtained by transmission electron microscopy (TEM) also at high resolution (HRTEM). The TEM instrument used was a JEOL-FS2200 with in column filter, at EMPA Laboratories. For the identification of the nature of the different non-carbonaceous PM, the X-Ray powder diffraction method (XRD) was applied.

5. Distribution and nature of PM in the DPFs

5.1. GFM-DPFs – Macroscopic and optical microscope observations

A common macroscopic feature of all three sectioned DPFs of this type is the widespread occurrence of a greenish coloured deposition material (Fig. 1), which is thickest at the corners of mainly the inlet channels. This is a primary characteristic acquired during the coating procedure. The greenish material is due to the V_2O_5/TiO_2 catalytic coating and is best distinguished in the B100-DPF (GFM4), as this shows the least amount of soot deposition. The very low amount of soot in the B100-DPF is evident already on a macroscopic scale (Fig. 1). Figure 1 depicts also the widespread soot deposition in the B20- and B0-DPFs.

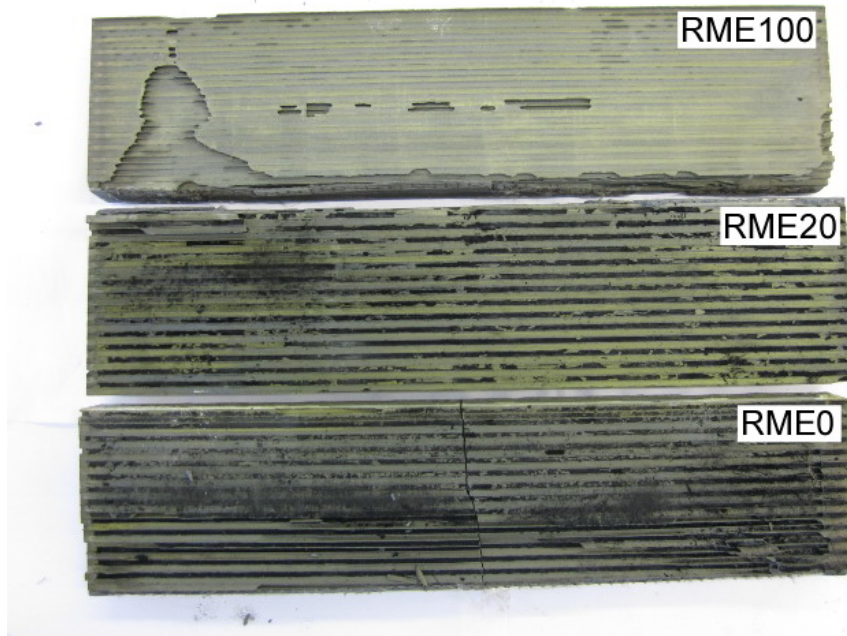


Fig. 1: Photograph of the interior part of the segments from the investigated GFM-DPFs showing the predominance of the green colour, due to the catalytic coating material, as well as the abundance of soot (black) in B20 (RME20) and B0 (RME0) DPFs.

Interestingly, the B100-DPF shows the highest amount of ash deposits, distinguished also macroscopically in form of a beige coloured powdery material accumulated at the plugged ends of the inlet channels, at the outflow side of the DPF (Fig. 2). Ash is filling up a length of about 15 mm of the ca. 300 mm long channels from the plugged ends toward the inlet. Within the ash deposits, considerable amounts of fibrous material are observed. As discussed later in this report, this fibrous material originates mainly from the gasket placed at the DPF front (inlet) side and was transported mechanically within the DPF by the exhaust stream.

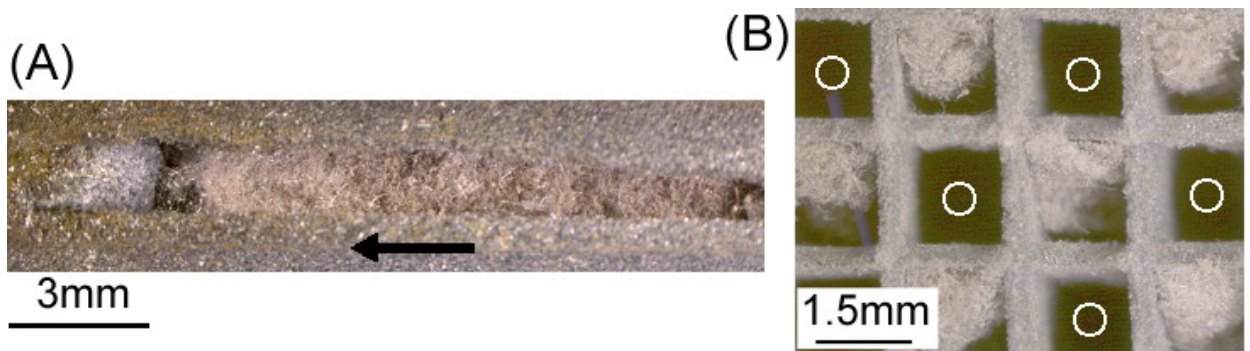


Fig. 2: Microphotographs of ash (beige colour) at the plugged ends of inflow channels in the GFM-B100-DPF; (A) parallel to the flow (arrow shows the flow direction); (B) perpendicular to the flow; O: outlet channels.

5.2. GFM-DPFs - SEM-results

5.2.1. Soot

The DPFs operating with both the B20, as well as the B0 fuel show deposition of a ca. 130-170 μm thick soot cake on the channel walls of only the inlet channels (Fig. 3). This is a feature observed commonly with DPFs operating with diesel fuel (e.g., [5], [1] and references therein). A soot cake is currently not observed on the channel walls of the B100-DPF (Fig. 3). However, loose pieces of a ca. 100 μm thick cake are found as pieces within inlet channels (Fig. 4). The shape of the soot cake fragments, in the form of a channel mould, indicates that it was originally deposited onto the channel walls but at some stage it has fallen off mechanically. The reason why the soot cake could not hold on the channel walls is probably related to the nature and amount of the underlying material (see below).

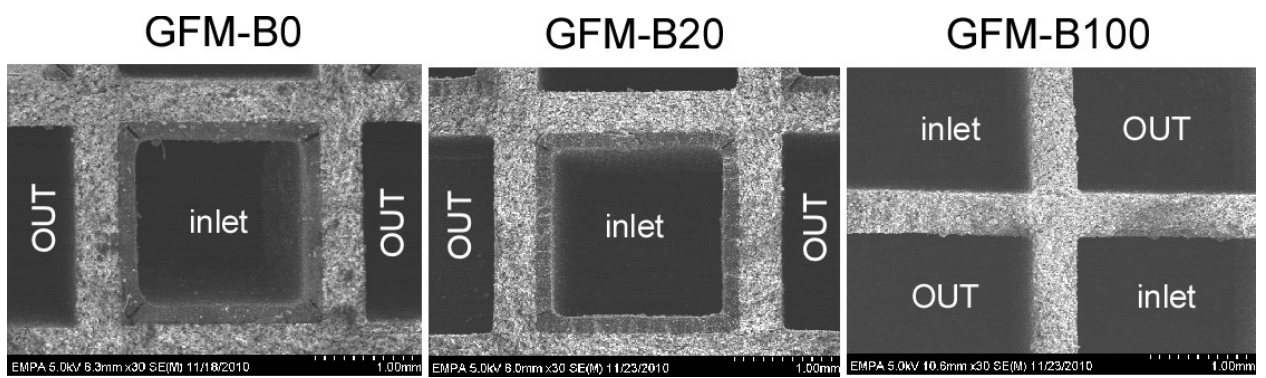


Fig. 3: Secondary electron (SE) SEM images of in- and outlet channels of the three GFM-DPFs showing a ca. 130-170 μm thick soot cake deposited at the inlet channels along the whole filter length of the B0- and B20-DPFs. The B100-DPF shows no soot cake deposition on the channel walls any more (see text for details).

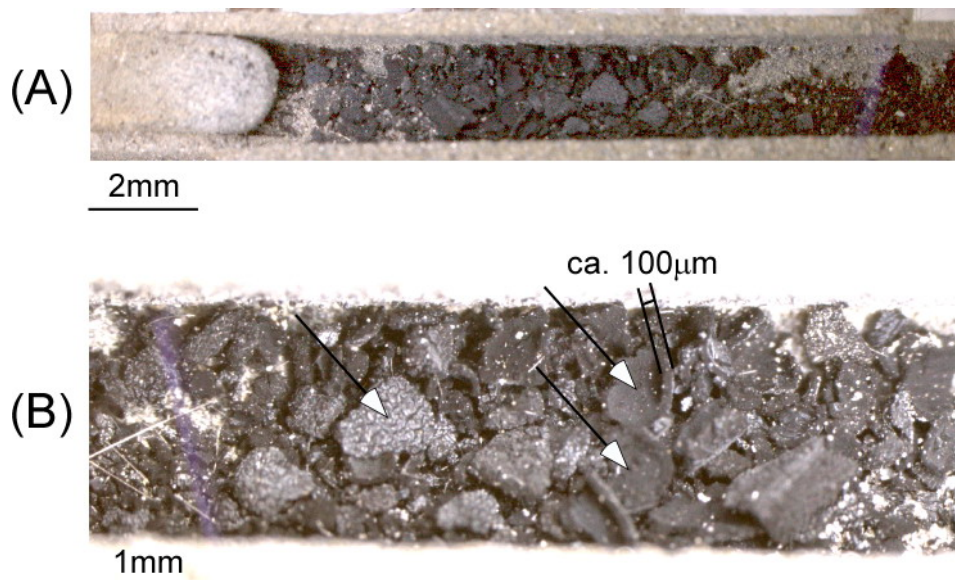


Fig. 4: Microphotographs of loose soot fragments accumulated toward the plugged ends of the inlet channels in GFM-B100. (B) exhibits a detail of (A) and shows the shape of the soot fragments, which corresponds to the mould of inlet channels (best distinguished at the fragments pointed by arrows). The leftmost arrow shows the back side of a soot cake piece facing the channel wall.

5.2.2. Ash

As already mentioned earlier, the highest amount of ash is observed at the plugged ends of the inlet channels only in the B100-DPF. Lower amounts of ash are observed also onto the channel walls of the same DPF. The B20 and B0 filters show no ash deposits at the plugged ends. However, some ash material occurs underneath the soot cake (Fig. 5B-C) with B20 and only minor ash deposits in combination with B0 (Fig. 5D). Abundant long-prismatic crystals, the nature of which is discussed later under 'other particles', occur mixed with the ash at these sites.

EDX analyses of the ash reveals that it consists of the following elements: Ca, S, P, O, Mg, K and minor Zn, V, Ti, W, Al, Si, Na, Fe and Cu. The material deposited on the channel walls underneath the soot cake contains mainly V, Ti, O, Al, Si, minor P, Na, W, Fe, K and traces of Ca and therefore consists of ash *sensu stricto* (produced during the combustion process) mixed with some other components.

Tracing back the elements identified in the deposition material as described above, V, Ti and W come from the catalytic coating, Fe and Cu from engine wear and Ca, P, Zn, Mg, S and Na from the fuel and the lube oil. Thus, ash deposition at the channel walls seems to be intermingled together with material of the catalytic coating layer. The origin of Al and Si is addressed below under 'other particles'. Interestingly, the higher amounts of ash and higher

proportion of Ca in especially in the B100 but also in B20, compared to the B0-DPF indicate that the biofuel is an important source of ash.

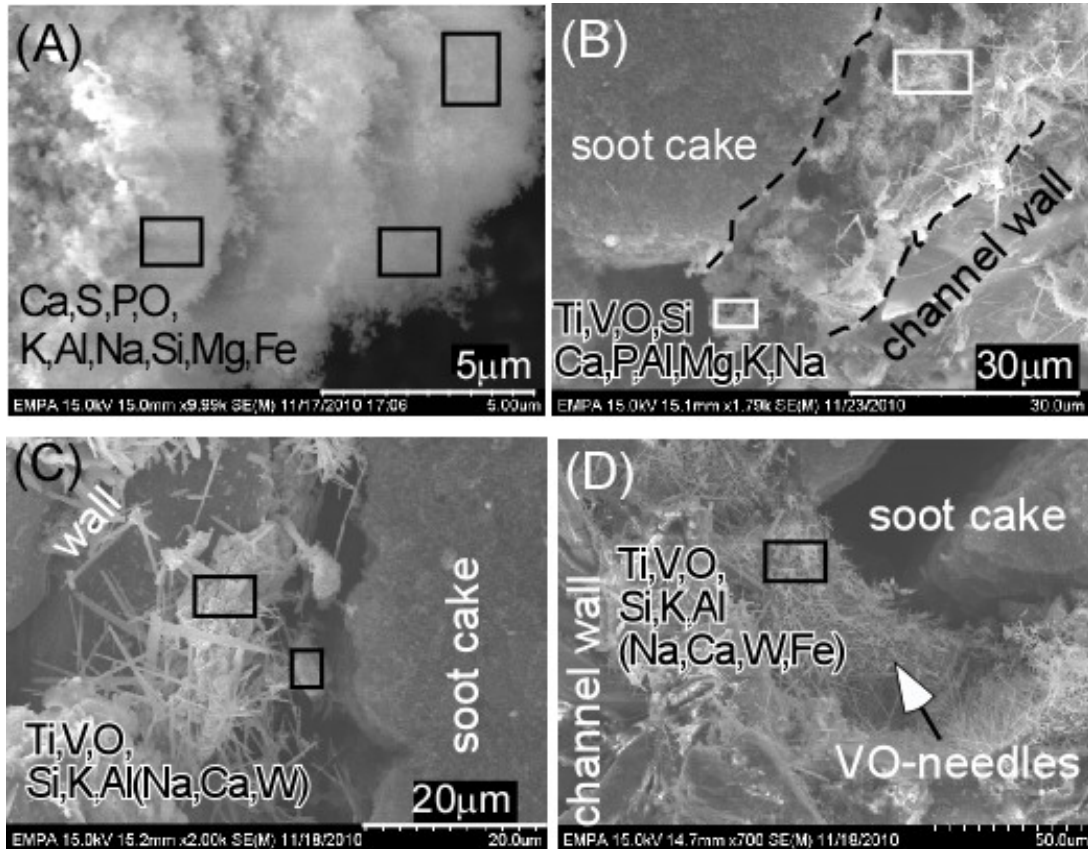


Fig. 5: SE-SEM images of (A): ash accumulated at the plugged ends of GFM-B100; (B, C): ash and coating material on channel walls between soot cake and channel wall of GFM-B20 and (D): GFM-B0. Rectangles mark the sites analysed by EDX. Elements in parenthesis occur in minor amounts. Dashed line in (B) marks the limits between soot cake and channel wall, for clarity.

5.2.3. Other particles

Apart from the soot and ash (*sensu stricto*), some other particles are observed among the PM deposition material observed within the studied DPFs. These particles occur together with the ash deposits and/or attached to soot agglomerates. They include:

- (a) Approximately 30-100 nm wide and up to a couple of μm long, needle-shaped particles widespread mainly within fissures of the catalytic coating layer, as well as on the catalytic layer surface itself (Fig. 6A-C). Numerous such long needles are observed also underlying the soot cake, especially at the channel corners, either as isolated crystals or mechanically mixed with the ash. EDX analyses of such isolated crystals reveal the presence of V and O.

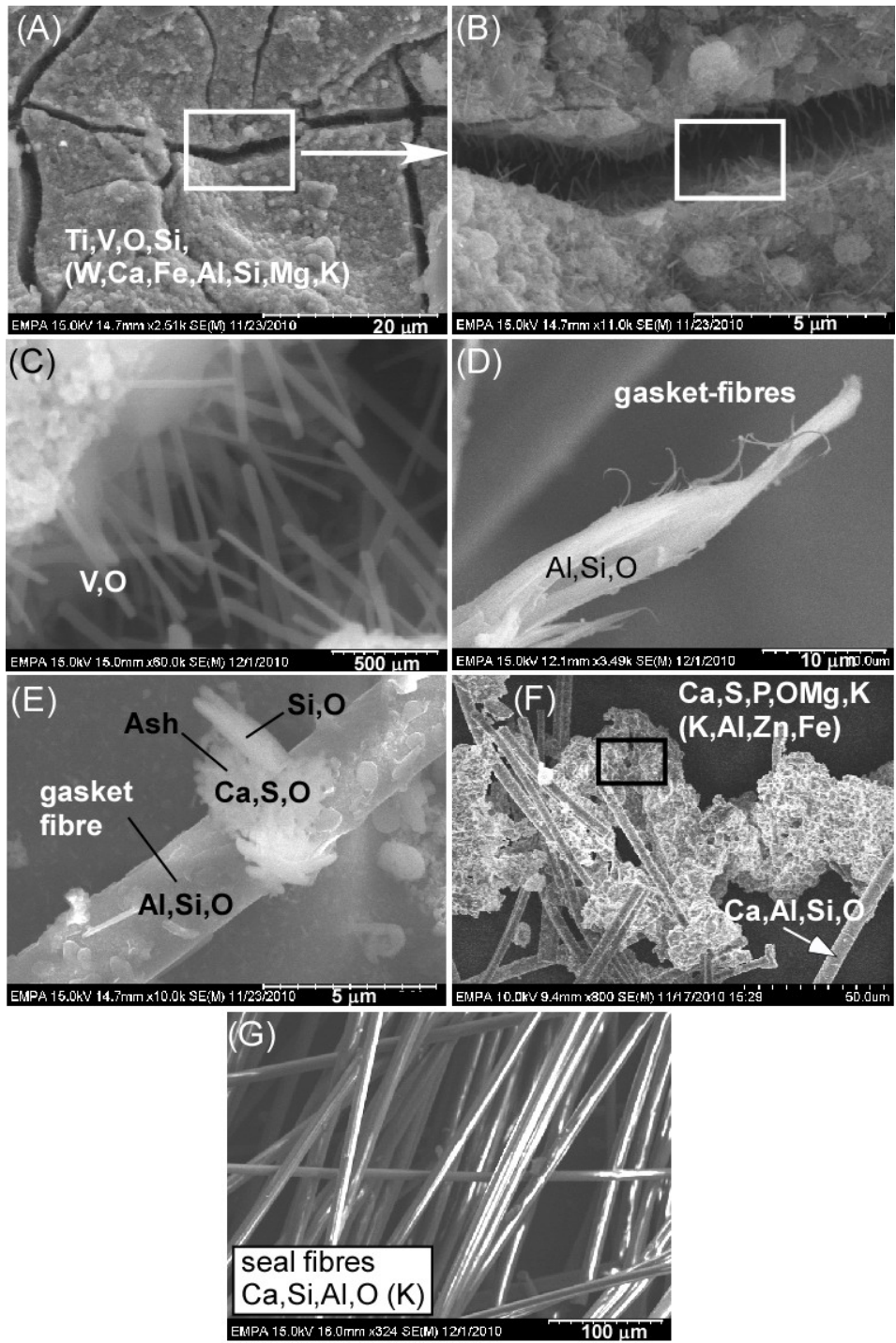


Fig. 6: SE-SEM images of different particles other than soot and ash in the GFM-DPFs. (A): fissures in the catalytic coating layer where V-O-bearing long prismatic crystals occur; (B) is a magnification of the rectangle in (A); (C) is a magnification of the rectangle in (B); (D): Al-Si-O-fibres taken from the gasket on the DPF inlet surface; (E) a single Al-Si-O gasket fiber with ash and Si-O-crystals inside the DPF; (F) Ca-Si-Al-O fibers from the intumescing mat mixed with ash; (G) Ca-Si-Al-O fibers taken from the intumescing mat for comparison. The rectangle in (F) marks the site analysed by EDX.

High magnification images show that the V-O-needles are long-prismatic crystals. This feature, combined with their mode of occurrence in close association with the catalytic coating layer, as well as their chemical composition, imply that they grew newly at some

stage of the DPF operation. Especially their appearance perpendicular to the walls of fissures present in the catalytic coating layer clearly shows that they are newly formed at these sites. Based on the chemical composition, the needles are V-oxides, where V is probably in a lower oxidation state compared to that in the original V_2O_5 .

(b) Approximately 100-200 nm wide and variably long (up to several μm) fibres. Based on EDX analyses, they consist of Al, Si and O and very probably originate from the gasket at the outer inlet surface of the DPF. SEM imaging of samples taken from a new gasket, identical to that used in the aftertreatment assembly during the tests, reveals that when heated to ca. 200 °C, the gasket disintegrates to a fibrous material with the same chemical and morphological characteristics as the fibers found intermingled with ash (Fig. 6 D, E). The width of the fibers may vary depending on the degree of disintegration of the gasket material (Fig. 6D). It is noted that the use if this gasket was in combination with only this particular experimental setup.

(c) Approximately 10 μm wide and several μm long fibres (Fig. 6F). These fibres are much wider than the Al, Si, O ones from the gasket and have a different chemical composition, in that they consist of Ca, Al, Si and O (EDX data). Examination of the material used as insulation medium enveloping the exhaust aftertreatment assembly (DPF \pm DOC) under the SEM reveals that it is composed of fibres with the same morphological characteristics and chemical composition (Fig. 6G). Thus, part of this material is probably detached at some stage from the intumescent seal and enters the DPF.

The characteristics of the deposition material found within the three GFM-DPFs are summarized below, Table 4.

5.3. GFM-DPFs – HRTEM imaging

As TEM has a higher resolution compared to SEM, it provides more detailed data on the inner structure of particles, down to the nanometer scale. It is widely accepted that soot from diesel engines commonly occurs as chain-like agglomerates composed of numerous primary particles with a nearly spherical shape and diameters mostly of a few tens of nanometers. The agglomerates consist of graphene segments comprising several polyaromatic hydrocarbons (PAH). It is reminded that graphenes are one atom thick planar layers of carbon in a honey comb structure.

Table 4: Summary of the main characteristics of PM deposited inside the GFM-DPFs

	B100	B20	B0
Soot amount	Little	much	much
Soot cake	ca. 100 μ m thick (as loose fragments - not on channel walls)	130-170 μ m thick (on channel walls)	130-170 μ m thick (on channel walls)
Ash amount	Substantial	very little	very little
Ash distribution	- at plugged ends of inlet channels, - on channel walls	on channel walls	on channel walls
Chemistry of ash (by EDX)	Ca,S,P,O,Mg,K (Zn,Al,Si,Na,Fe,Cu) ¹	Ca,S,P,O,Mg,K (Zn,Al,Si,Na,Fe,Cu)	V,Ti,O,Al,Si (P,Na,Fe,Ca)
Chemistry of other particles (by EDX)	VO-needles (coating medium) ² Al,Si,O fibres (gasket) Ca,Al,Si,O fibres (insulating seal)	VO-needles Al,Si,O fibres Ca,Al,Si,O fibres	VO-needles Al,Si,O fibres Ca,Al,Si,O fibres

¹Elements in parenthesis are found in minor amounts;

²The terms in parenthesis indicate the origin of the particles.

Various TEM studies report that the internal structure of diesel soot individual particles is characterized by the presence of graphene layers of variable length and degree of curvature (e.g. [6, 7]). The graphene layers constituting the soot individual particles show locally more or less regular arrangements and a various degrees of ordering. The innermost part of the soot spherical particles is generally interpreted as more or less amorphous.

The degree of order of such structures strongly depends on temperature, as well as on the fuel of origin (e.g., [8]) and affects the oxidative behavior of soot. Oxidation preferably removes amorphous carbon relative to graphitic carbon. The length, degree of curvature and degree of crystalline order of the graphene layers are parameters reflecting the oxidative reactivity of the soot. The oxidative reactivity of soot depends also on the size of the particles (surface to volume ratio), as well as on the surface structure, i.e. on the presence of the so-called functional groups on the surface and number of edge sites. Thus, a curved graphene layer, for instance, has more edge sites than a straight one and shows therefore a higher degree of reactivity. Thus, the internal nanostructure of soot particles is a measure of its oxidative reactivity.

The TEM study carried out on the soot deposited in the B100-DPF confirms most of the above described general characteristics for diesel soot. The size of the soot spherical particles ranges between 11 nm and 38 nm in diameter with a mean value of 21 nm and a standard deviation of 6 nm for a total of 101 measurements (Fig. 7). With this mean diameter

size, the B100 soot particles are rather on the low side compared to values reported for diesel soot particles (e.g., [8]).

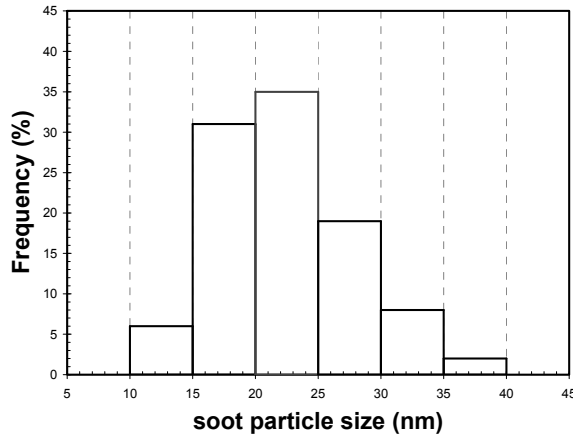


Fig. 7: Histogram showing the size distribution of the individual soot particles (particle diameter) in the soot agglomerates of GFM-B100 (101 measurements, based on TEM images)

Regarding their internal nanostructure, the soot particles of the B100-DPF exhibit two parts with distinct features (Fig. 8): (a) a larger outer part, usually constituting about 2/3 of the whole size of the particle sphere, where graphene layers are arranged sub-parallel and locally parallel to each other (e.g. white rectangle in Fig. 8A) forming nm-thick packages interrupted by less ordered material and (b) a smaller innermost part with a relatively random arrangement of shorter graphene layers (marked by the dashed line in Fig. 8B).

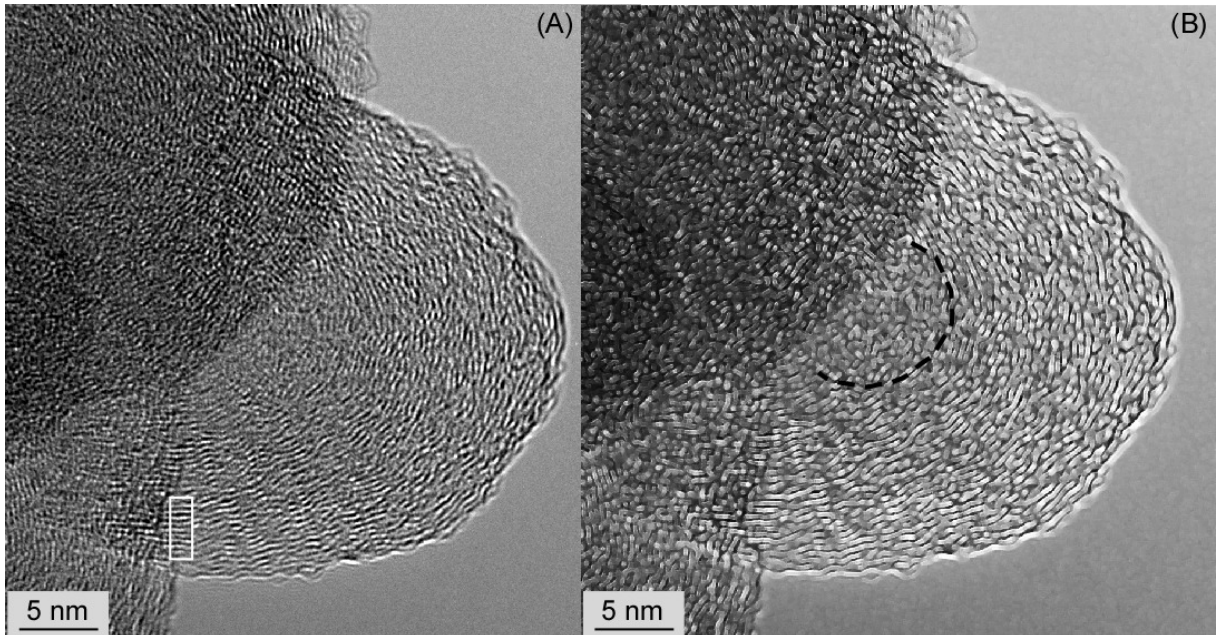


Fig. 8: HRTEM images of a representative soot particle from the GFM-B100-DPF. In (B) the image is processed in 'Photoshop' by applying the filter 'Brush strokes – accented edges', which renders the fringes arrangement more discernible. The dashed line marks the particle core with a more amorphous structure.

The graphenes at the outer particle part are a few nm long with a slight curvature giving rise usually to a wavy shape. In general, the graphene layers length increases and their degree of curvature decreases toward the outer particle part. These features reflect a decrease of the oxidative reactivity of the soot spherical particles toward the outer particle part. Locally, a higher degree of crystalline order is observed by regular repetition of graphenes (up to 10 alternating layers in 1-2 nm wide packages) in a crystalline (graphite-like) structure.

It has to be brought in mind that the TEM images depict projections of the whole spherical particle on a plane. Thus, the imaging characteristics obtained by HRTEM for the innermost part of the soot spherical particles, where the sphere is thickest, are less detailed and less straightforward to interpret compared to those of the outer parts. Therefore, there is a degree of uncertainty concerning the interpretation of the graphene layers disorder for the central part of the particle. Assuming that the information about the random arrangement of graphenes in the particle core is more or less close to reality, the core reflects a higher oxidation capacity compared to the outer parts and implies that soot is easier oxidized during the initial stages of its formation and develops a higher degree of carbon atoms ordering during further residence time in the exhaust gas and in the DPF deposits.

Compared to the nanostructure of diesel soot (e.g. [6, 1]), the above described characteristics of the biodiesel soot imply a slightly higher oxidation capacity of the latter. This inference is in line with previous results (e.g., [9]).

5.4. SFM-DPFs – Macroscopic and optical microscope observations

Macroscopic observations of the sectioned DPFs reveal that in B0 and B20 considerable amounts of soot were deposited on the channel walls of the inlet channels, along about 15-20 cm of the ca. 30 cm long channels (from the outlet toward the inlet side). The B100-DPF shows hardly any obvious soot depositions. Only minor amounts of soot are observed by optical microscopy onto the channel walls. This difference in soot amount depositions in the SFM-B100 compared to the GFM-B100-DPF described earlier (section 5.1.) is probably due to the significantly higher temperatures experienced by the SFM- B100, which lead to almost complete oxidation of any soot depositions. Macro- and microscopic studies of the B100-DPF reveal melting phenomena: transparent spherical particles of up to 1.5 mm in diameter and/or transparent droplets are widespread in this DPF (Fig. 9A), the deposition material on the channel walls has a glassy appearance (Fig. 9B) and part of the filter interior shows a rounded surface (Fig. 9C). These characteristics are related to the unusually high

temperatures experienced by this DPF, which must have exceeded by far the 1200 °C given by the prescriptions (see below).

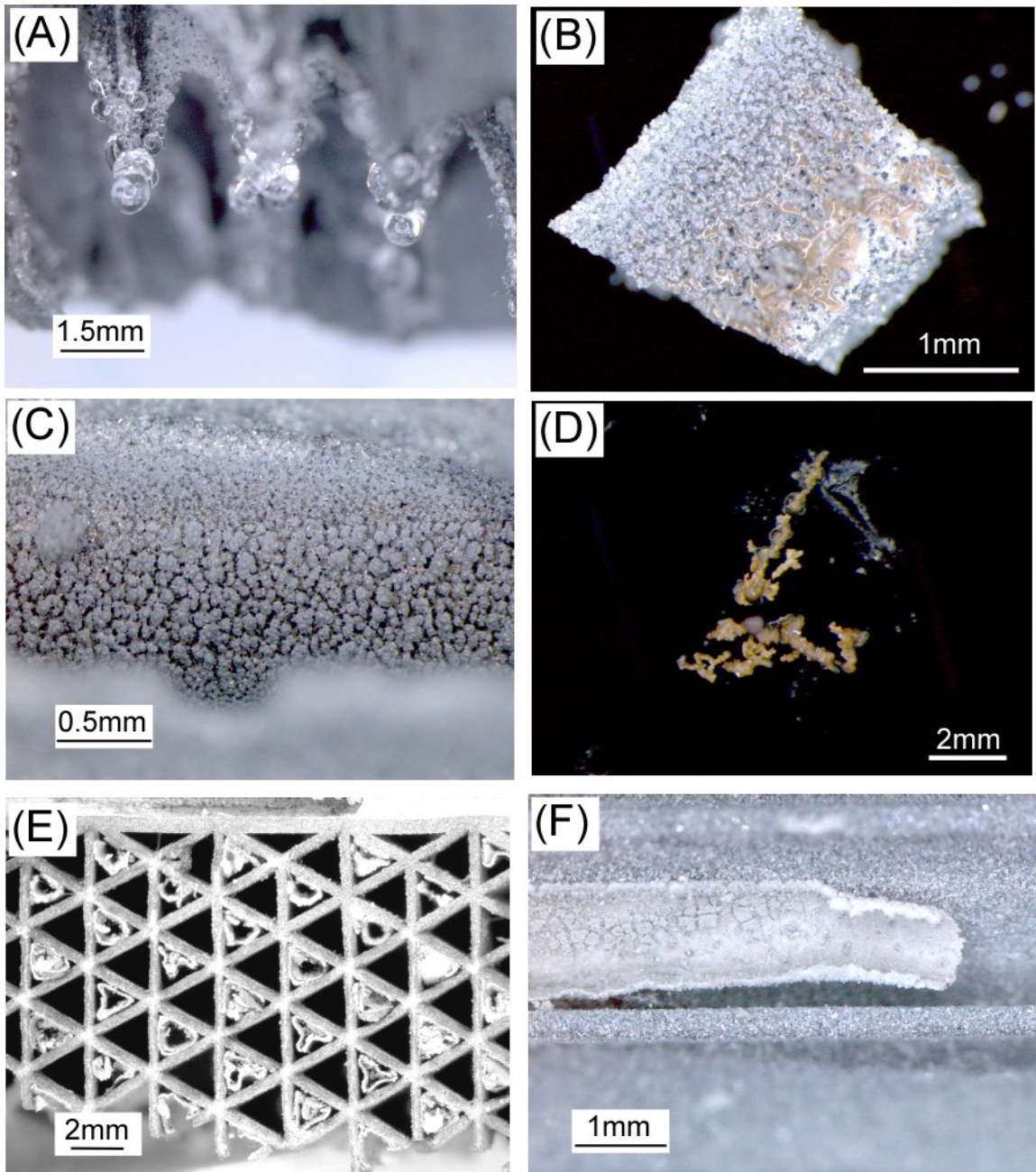


Fig. 9: Microphotographs from the SFM-B100-DPF showing various formations resulting by melting (A-D); (A): transparent spherical particles at the channel walls; (B) a channel wall slab with deposition material melted and incorporated on the channel wall (brown: melted ash); (C) surface of a channel wall slab with a rounded surfaces, due to partial melting; (D): melted brown ash loose aggregates; (E): cross section of the part of the DPF close to the outlet showing deposition of a grayish layer in the inlet channels; (F) part of an inlet channel parallel to the flow direction with deposition of a ca. 60µm thick grayish layer.

Ash depositions are macroscopically not obvious, neither in the B0 nor in the B20 DPF. The B100-DPF shows no ash accumulation at the plugged ends of the inlet channels but rather random depositions of small amounts of brown coloured ash aggregates with a glassy appearance in the inlet channels, not attached on the filter walls (Fig. 9D), as well as incorporated on the filter walls themselves after melting (Fig. 9B).

Interestingly, a ca. 60 μm thick grayish layer is observed along at least the half length of the inlet channels to the outlet side of the B100-DPF (Fig. 9E, F). The nature and origin of this layer is discussed later under 5.5 ('other particles').

5.5. SFM-DPFs - SEM-results

5.5.1. Soot

The DPFs operating with both the B0, as well as the B20 fuel show deposition of a ca. 200 μm thick (or thicker) soot cake on the channel walls of the inlet channels along ca. 2/3 of the whole DPF length, toward the outlet (Fig. 10). The soot cake depositions lead to almost complete channel blockage in the last 40% of the DPF, toward the outlet. Soot depositions in form of a cake were not observed in the B100-DPF (Fig. 10). Only traces of soot agglomerates were found in this DPF, randomly distributed on the channel walls of the inlet channels.

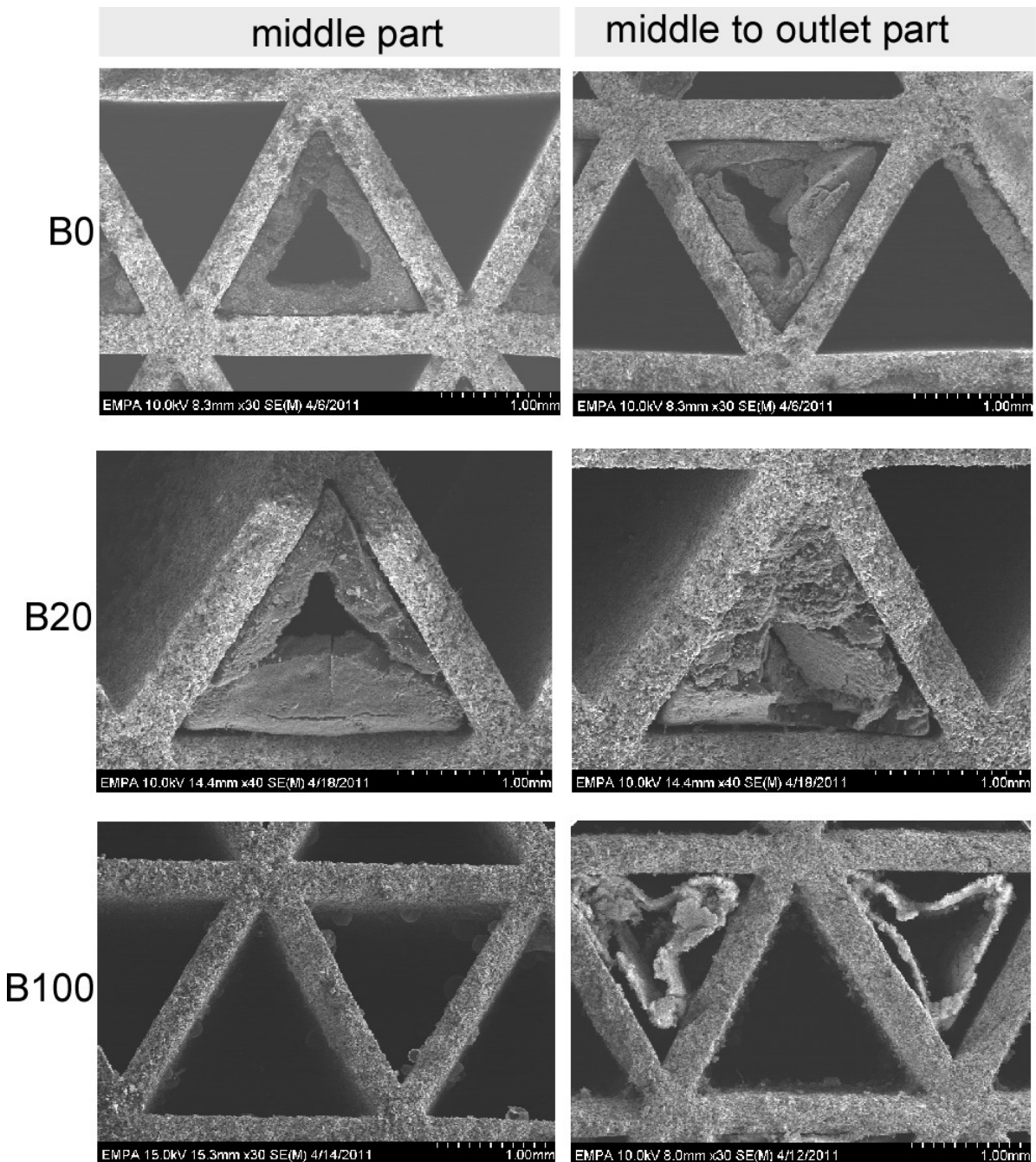


Fig. 10: SE-SEM images from the SFM-B0-, B20- and B100-DPF showing soot cake depositions in the inlet channels of B0 and B20. The B100-DPF shows no soot cake depositions but a ca. 60 μ m thick grayish layer at the middle to outlet side.

5.5.2. Ash

In general, very little ash was deposited in all three investigated DPFs. The highest ash amount occurs in B100 but, due to the increased temperatures developed in this filter during regeneration, the original form of ash depositions has been obscured. Brown ash deposits in B100 have currently a glassy appearance indicating that the ash agglomerates, at least partly, melted. EDX analyses of the ash revealed mainly Ca, P, O, minor S, Zn, Na, Al and Si (Fig. 11A).

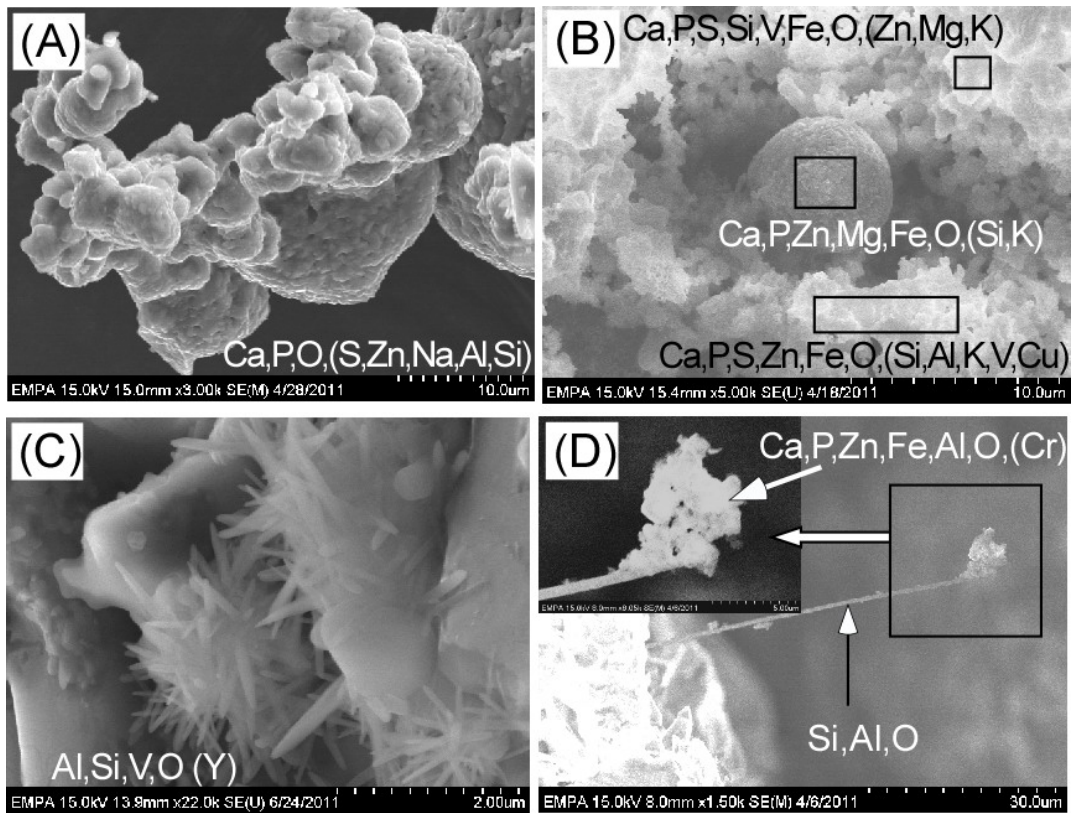


Fig. 11: SE-SEM images from the SFM-DPFs showing ash agglomerates with variable composition. (A) is from B100, (B,C) from B20 and (D) from B0. In (D), an ash agglomerate is holding on an Al-Si-O fiber. Rectangles indicate the sites analysed by EDX. Elements in parenthesis occur in minor amounts.

In B20 and B0, ash was detected on the channel walls, underneath the soot cake, where this was present. In B20, ash deposits seem to be a little more abundant than in B0. They form agglomerates (particles held loosely to each other) but also aggregates (firmly held particles) of crystalline phases consisting of Ca, P, O, Zn, \pm S, \pm Mg, \pm V, Fe, Si, Al and minor K, Cu, Ni or more rarely P, Ti, V, Al, Si, Fe (Fig. 11B, C). Newly formed crystals and crystal aggregates of Al, Si, O, V composition, occasionally with minor Y, were observed locally (Fig. 11C). In B0 only a few ash agglomerates were found, which consist of Ca, P, Zn, Fe, Al and minor Cr (Fig. 11D).

5.5.3. Other particles

(a) Fibers: Fibers were observed in all three investigated DPFs, especially at the inlet channel ends (Fig. 12A). Two types of fibers are distinguished, based on their chemical composition, as obtained by EDX analyses: (1) Si-Al-O, occurring mainly at the outlet part and in lesser amounts also in the middle part of the DPF (Fig. 12A). They are approximately 100-200 nm (up to a few μm) wide (Fig. 12B) and variably long (up to several μm). Similar to the GFM filters, they very probably originate from the gasket at the outer inlet surface of the

DPFS. (2) Si-Al-Ca-O fibers, approximately 100-300 nm (up to a couple of μm) wide and variably long, up to several μm . In B100, they are locally molten forming drop-like to spherical particles all along the fiber main body, as well as at the fiber ends (Fig. 12C, D). Their Ca-Al-Si-O composition corresponds to that of the intumescing mat used as insulating material around the outer DPF surface. The unusually high temperatures developed during regeneration of B100 are probably responsible for partial melting of the intumescing mat fibrous material.

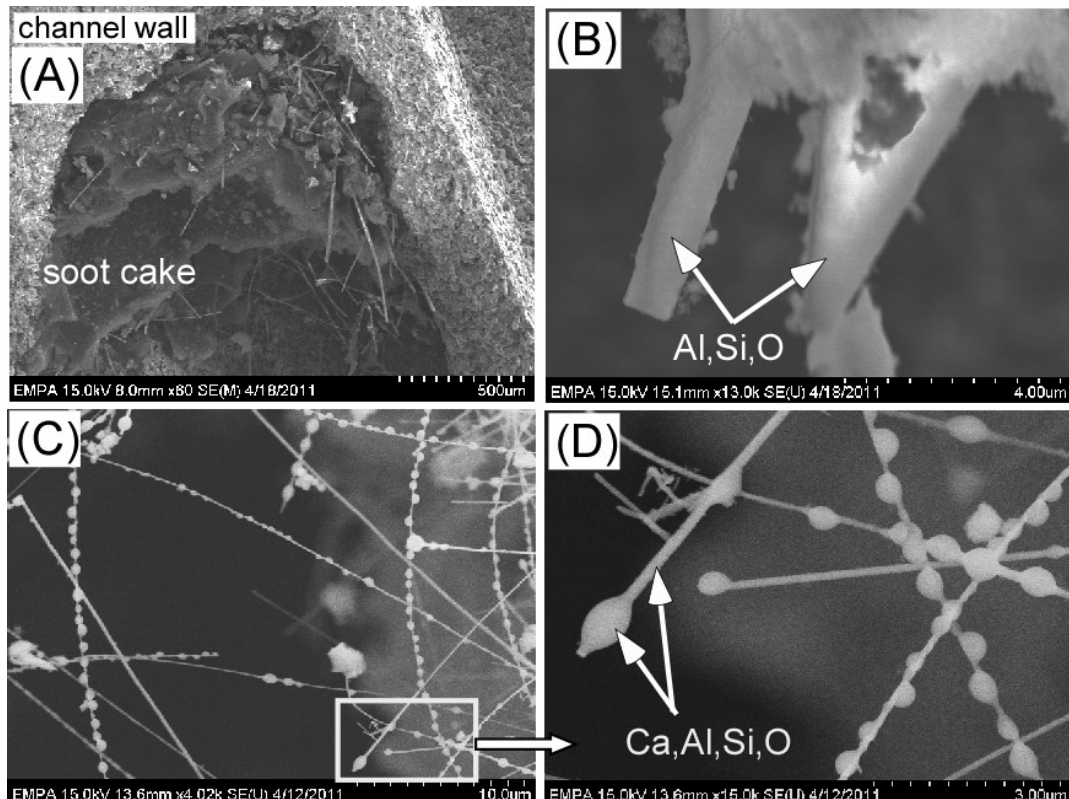


Fig. 12: SE-SEM images from the SFM-DPFs showing: (A): Al-Si-O and Ca-Al-Si-O fibers at the inlet channel ends of both the B20- and B0-DPF; (B) Si-Al-O fibers from the gasket with attached ash agglomerates at the uppermost part of the image; (C, D): Ca-Al-Si-O fibers melted locally in drop-like forming shapes from the B100-DPF. (D) is a magnification of the rectangle in (C).

(b) A ca. 60 μm thick grayish layer is observed along at least the half length of the inlet channels to the outlet side of the B100-DPF (see also above, under 5.4.). SEM imaging reveals that this layer mostly consists of a fibrous network and lesser amounts of accumulated round pellets (Fig. 13A-C). EDX analyses of both fibers and pellets show the elements Si, C and minor O. High magnification images of the fibers reveal that, at least part of them, consist of numerous individual pellets accumulated over each other in pile-forming shapes giving rise to a needle-like appearance (Fig. 13C). X-ray powder diffraction analyses of this material yield peaks well coinciding with the mineral moissanite (SiC), as well as minor amounts of quartz (SiO_2). Based on the X-Ray diffraction results, in combination with the chemical composition obtained by EDX analyses, it is inferred that the grayish layers form

from the SiC filter material at very high temperatures. (c) Transparent, glassy rounded particles of up to 1.5 mm in diameter in the B100-DPF (Fig. 13D; see also above under 5.4.). High magnification SEM images reveal that the surface of these particles consists itself of numerous smaller rounded spherules (Fig. 13E). EDX analyses reveal the elements Si, C and minor O. X-ray powder diffraction analyses show that this material is not amorphous glass but consists of crystalline material and yields peaks identical to the ones obtained by the grayish layer, that is well coinciding with the mineral moissanite (SiC), as well as minor amounts of quartz (SiO_2). Similar to the grayish layers described above, the transparent rounded particles probably form from the SiC filter material during the very high temperatures of regeneration. Considering that the melting temperature of SiC is close to 2000 °C and taking into account melting appearances on the DPF wall material itself (rounded SiC surfaces in parts of the filter, especially close to the outlet side) it is presumed that this DPF must have seen locally such high temperatures.

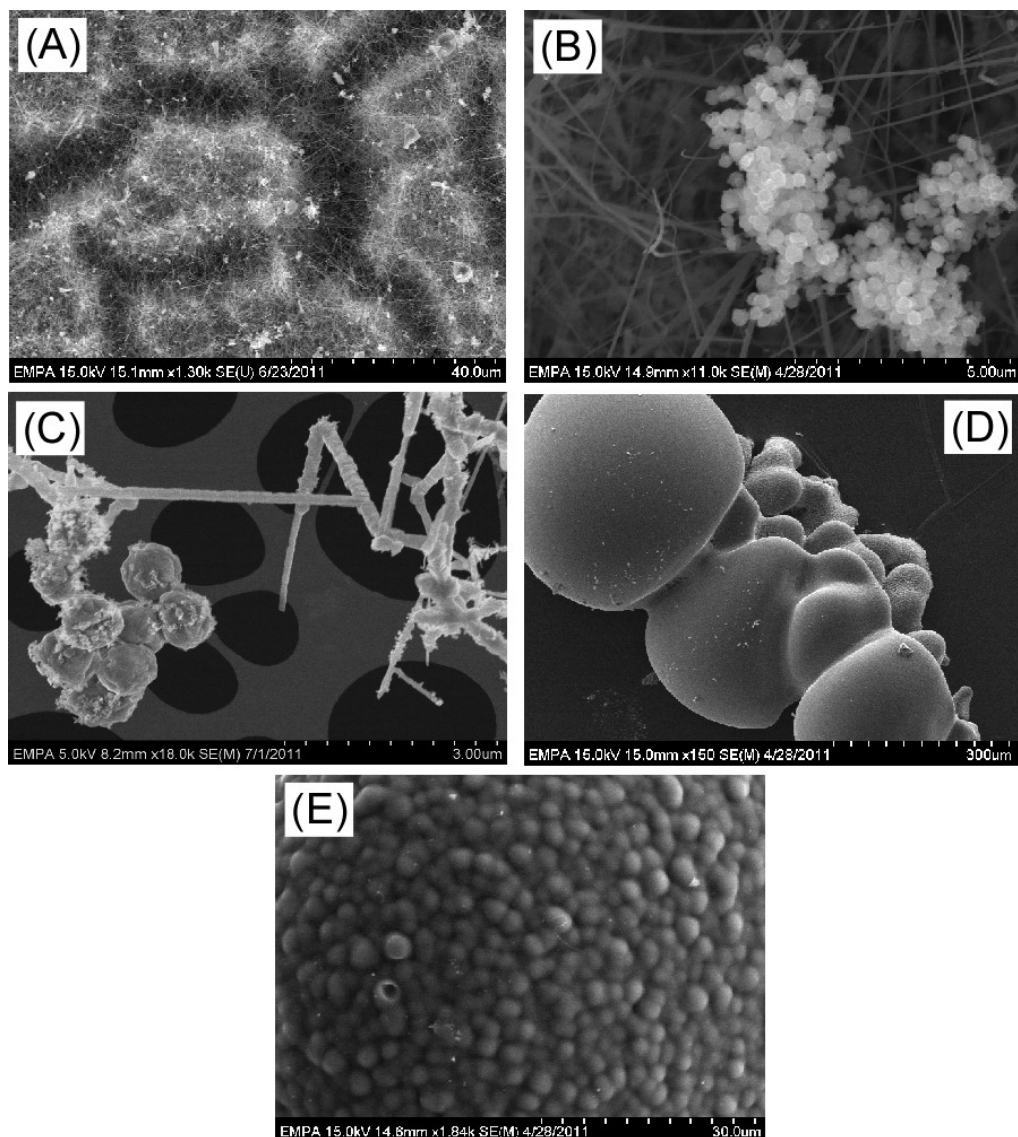


Fig. 13: SE-SEM images from the SFM-B100-DPF showing: (A-C): the structure of the greyish layer deposited in inlet channels consisting of fibers and pellets with a SiC composition. In (C) pilling-up of individual pellets gives rise to a needle-like appearance, best evident on

the right side of the apparent letter 'A'; (D, E): transparent SiC round particles. E is a detail of the surface of one round particle in (D).

5.5.3. Additional observations of the DPF wall material

All three examined DPFs show needle-like to worm-like formations, commonly attached on the channel walls, especially at the SiC wall grain boundaries (Fig. 14A-G). The needles have commonly a spherical end (Fig. 14B, D). Chemically, these formations consist of mainly Si but variable proportions of Al, O and C may occur occasionally. The mode of occurrence of these particles attached to the channel wall material, as well as their predominantly Si-rich composition indicate that their formation is mainly related to the SiC wall material rather than to external sources but at this stage of investigation a safe conclusion cannot be drawn.

The amount and length of these formations are most pronounced in the B100-DPF, which has seen the highest temperatures (Fig. 14H).

The characteristics of the particles found within the three SFM-DPFs are summarized below, in Table 5.

Table 5: Summary of the main characteristics of PM deposited inside the SFM-DPFs

	B100	B20	B0
Soot amount	traces	much	much
Soot cake	no – only a few soot agglomerates on inlet channel walls	≥ ca. 200 µm thick on inlet channel walls up to complete channel blockage	≥ ca. 200 µm thick on inlet channel walls up to complete channel blockage
Ash amount	little (often melted)	very little	very little
Ash distribution	random - melted aggregates	on channel walls	on channel walls
Ash chemistry (by EDX)	Ca,P,O,(S,Zn,Na,Al,Si) ¹	Ca,P,O,Zn,S,Mg,V,Fe, Si,Al,(K,Y,Cu,Ni)	Ca,P,Zn,Fe,Al,O, (Cr)
Other particles	-Al, Si, O fibers (gasket) ² -Ca, Al, Si, O fibers (insulating seal) -Si, (Al, O, C) needle- and worm-like formations (channel wall) -Si(O, C) grayish layer (channe wall) -Si(O, C) transp. round particles (channel wall)	-Al, Si, O fibers -Ca, Al, Si, O fibers -Si, (Al, O, C) needle- and worm-like formations	-Al, Si, O fibers -Ca, Al, Si, O fibers -Si, (Al, O, C)) needle- and worm-like formations

¹Elements in parenthesis are found in minor amounts; ²The terms in parenthesis indicate the origin of the particles.

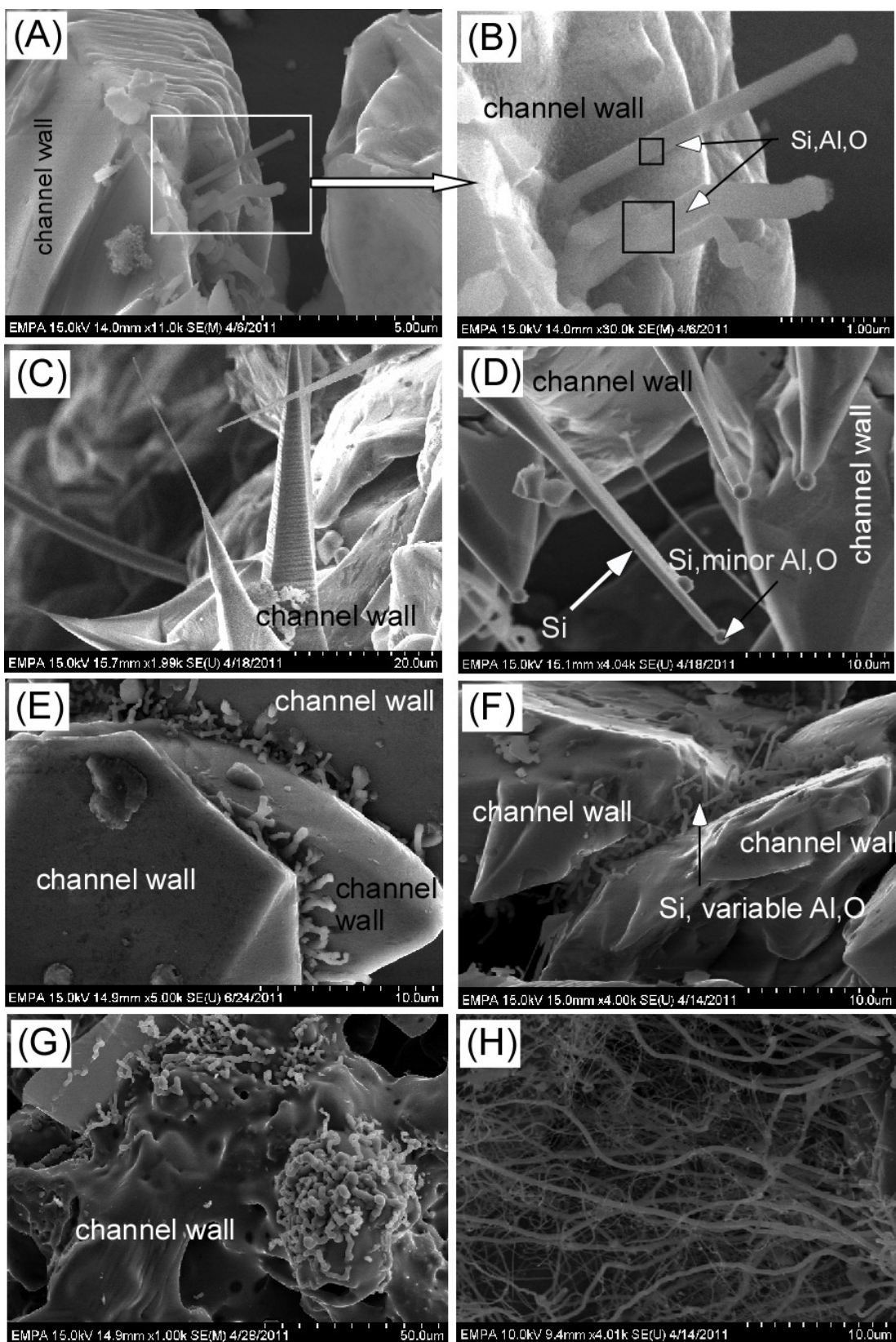


Fig. 14: SE-SEM images from the SFM-DPFs. (A-F) are from the B20 and B20 and show needle-like to wormy formations attached on the channel wall, mostly with a spherical head. The needles are partly evolving from larger, prismatic formations at the channel wall (C, D); (G, H) are from the B100 and show a dense network of fibrous SiC material.

6. Conclusions

Based on the macroscopic and microscopic investigations (optical microscope, SEM, HRTEM), as well as X-Ray diffraction analyses of PM deposited in two different DPF-types (GFM-B100, GFM-B20, GFM-B0, as well as SFM-B100, SFM-B20, SFM-B0) operating on the same engine, the following conclusions can be drawn¹:

1. The B100-DPFs show very little soot deposition, opposite to B20 and B0 which exhibit abundant soot deposits. This observation applies for both GFM and SFM types of DPF.
2. Soot in all three GFM-DPFs, as well as in SFM-B20 and SFM-B0 forms a cake deposited on the channel walls. In GFM-B100, the soot cake is thinnest (100 µm) and at some stage it cannot hold on the walls of the channels, probably because of the nature and amount of the underlying material composed of ash and other particle components related to the catalytic coating and/or mechanically transported fibers. SFM-B100 shows hardly any soot deposition.
3. The average size of the individual soot particles in GFM-B100 is 21 nm (mean value of 101 measurements) with minimum and maximum values of 11 and 38 nm, comparable and rather on the low side in relation to pure diesel soot.
4. The size and internal nanostructure of the individual particles of GFM-B100 soot, as obtained by HRTEM images, reveal a relatively higher oxidative reactivity compared to diesel soot, as described in previous works.
5. The B100-DPFs contain significantly more ash compared to B20 and B0 implying that besides lubricating oil, RME-biofuel is the major contributor of ash production. This observation is more pronounced with the GFM-B100-DPF type, probably because the extremely high temperatures experienced by the SFM-B100-DPF obscured the original PM deposition material in this filter.
6. In the B0- and B20-DPFs of both GFM and SFM types, ash occurs onto the channel walls underneath the soot cake. Ash is found on the channel walls of GFM-B100-DPF implying that it occurred also underneath the thinner soot cake, which was originally deposited on the channel walls.

¹ Note: Observations of PM depositions and/or other observations in the SFM-B100 DPF (SFM5) are strongly related to the extremely high temperatures experienced by this filter (possibly reaching locally ca. 2000 °C) and cannot be generally considered as representative.

7. Newly formed V-O-bearing long prismatic nanocrystals occur in abundance within fissures of the catalytic coating layer, as well as on the coating layer surface in both inlet and outlet channels of all three GFM-DPFs. Their size and shape is such that they can escape to the ambient air.
8. Al-Si-O, as well as Ca-Al-Si-O-fibres deriving from the gasket on the outer inlet surface of the DPF and the intumescing mat, respectively occur inside all six DPFs, often mechanically mixed with ash. In SFM-B100 the Ca-Al-Si-O-fibres are locally molten giving rise to droplet-like or nearly spherical formations.
9. Based on SEM images and EDX analyses, the material underlying the soot cake in the three GFM-DPFs, which are catalytically coated, consists of ash (Ca, S, P, O, Mg, K), coating material (Ti, V) and its V-O-long prismatic crystal products, as well as gasket (Al, Si, O) and intumescing mat (Ca, Al, Si, O) fibres. In the SFM-DPFs, the deposition material other than soot consists of ash (Ca, P, S, Zn, Si, Mg, K, Al, V, Y, O), gasket (Al, Si, O), as well as intumescing mat (Ca, Al, Si, O) fibers.
10. Needle-like to worm-like formations consisting mainly of Si and occasionally variable amounts of Al, O, C occur attached to the filter wall material of all three SFM-DPFs. Their formation is rather related to the SiC wall material.
11. In the SFM-B100-DPF, which has locally seen very high temperatures (>1200 °C, possibly on the order of 2000 °C), both filter material, as well as deposited ash PM and intumescing mat melted, at least partly. The filter material gave rise to secondary fibers, platy particles, as well as rounded transparent particles of SiC composition (moissanite; X-ray powder diffraction data).

References

- [1] Liati, A., Dimopoulos Eggenschwiler, P. - Combustion and Flame 157 (2010), 1658-1670.
- [2] Song, J., Alam, M., Boehman, A.L. - Combust. Sci. and Tech. 179 (2007), 1991-2037.
- [3] Tsolakis, A., Megaritis, A., Wyszynski, M.L., Theinno, K. - Energy 32 (2007) 2072-2080.
- [4] Wu, F., Wang, J., Chen, W., Shuai, S. - SAE Techn. Paper (2008), 2008-01-1812.
- [5] Bensaid, S., Marchisio, D.I., Russo, N., Fino, D. - Catal. Today 1475 (2009), 295-300.
- [6] Vander Wal, R.L., Tomasek, A.J.. - Combustion and Flame 134 (2003), 1-9.
- [7] Song, J., Alam, M. Boehman, A.L., Kim, U. - Combustion and Flame 146 (2006), 589-604.
- [8] Su, D.S., Jentoft, R.E., Müller, J.O., Rothe, D., Jacob, E. Simpson, C.D., Tomovic, Z., Müllen, K., Tsolakis, A., Megaritis, A., Wyszynski, M.L., Theinno, K. - Energy 32 (2007)
- [9] Boehman, A.L. Song, J., Alam. M. - Energy & Fuels 19 (2005), 1857-1864